Advanced Steel Construction – Vol. 19 No. 4 (2023) 375–382
DOI:10.18057/IJASC.2023.19.4.6

AN EXPERIMENTAL STUDY ON SEISMIC PERFORMANCE OF STEEL COMPOSITE BEAM-COLUMN RIGID JOINT AND BUCKLING RESTRAINED KNEE-BRACED JOINT

Feng Xu [1,*], Zhe Yuan [1], Na Liu [1], Zhen-Xing Li [1,2], Lian-Guang Jia [1] and Wei Xu [1]

[1] *School of Civil Engineering, Shenyang Jianzhu University, Shenyang 110168, China*
[2] *China Southern Airlines Co., Ltd., Shenyang Maintenance Base, Shenyang 110169, China*
** (Corresponding author: E-mail: cefxu@sjzu.edu.cn)*

ABSTRACT

This paper evaluates the seismic performance of conventional steel composite beam-column rigid joints, and a novel buckling restrained knee-braced joint (BRKBJ), considering the impact of the floor slab. A series of quasi-static comparative tests were conducted to analyze the failure mode, load-bearing capacity, hysteresis performance, and ductility of both types of joints. Our findings revealed that the hysteretic curve of the BRKBJ exhibits a robust and shuttle-like shape, suggesting an adequate energy dissipation performance. However, its yield displacement is relatively small. Conversely, there is a marginal increase in the yield displacement of the beam and column, along with a significant rise in the yield load when compared to the rigid joint. The ultimate load-bearing capacity increases by 32.6%, and the displacement under this ultimate load decreases by 19.2%. Furthermore, the equivalent viscous damping coefficient and the ductility coefficient see an increase of 14.5% and 21.6%, respectively. When damage occurs to the joint, the buckling restrained knee brace helps shift the plastic hinge outwards, safeguarding the beam-column joint. It was also observed that the impact of the buckling restrained knee brace on the hysteretic behavior of the composite beam-column rigid connection at the beam end during the tension phase is notably more than during the compression phase. The presence of a floor has minimal effect on the BRKBJ.

ARTICLE HISTORY

Received: 27 November 2022
Revised: 29 June 2023
Accepted: 27 August 2023

KEYWORDS

Steel structure;
Combined beam-column joint;
Buckling restrained knee brace;
Quasi-static test;
Seismic performance

1. Introduction

Buckling restrained knee-braced joint (BRKBJ) is a new type of joint installed near the joint of steel beam and frame column. Moreover, the buckling restrained sleeve is placed outside to prevent its buckling instability. The core plate of the knee brace is composed of a low-yield-point steel plate. Under a small earthquake load, the knee brace can improve the lateral stiffness of the structure and meet the lateral displacement requirements of steel structural systems. Under a large earthquake load, the knee brace core plate yields before the beam-column main component and dissipates the seismic energy through its plastic deformation with no damage to the main component. Thus, it overcomes the weakness of the traditional design. Additionally, the BRKBJ of a steel frame structure has the advantages of large stiffness and good ductility. A buckling restrained knee brace (BRKB) is small, easy to replace and repair after damage, and can be assembled on site. Note that a BRKB can be used as lateral force resistance and energy dissipation component in the reinforcement and reconstruction of existing steel structures.

BRKBs of steel frames and joints have been studied theoretically and experimentally. Hsu and Li [1] studied the steel frame with an I-shaped steel knee brace. The results indicate that incorporating a knee brace enhances the load-bearing capacity of steel frame structures, although out-of-plane instability remains a significant concern. Junda et al. [2] investigated the seismic behavior of hinged steel structures with viscous damping knee brace joints. The results show that the viscous damping knee brace can remarkably improve the energy dissipation capacity of the frame. Yin et al. [3] proposed a double-tube BRKB system that can be employed in steel frame structures. This knee-braced system is founded on a cast steel connection. The author demonstrated the advantages of using a ductile cast steel material to enhance the energy dissipation of the buckling restrained brace. Chen et al. [4] analyzed the energy dissipation performance of a BRKB in bridge engineering, concluding that it effectively mitigates earthquake damage. Zhou [5,6] studied the angle, length, stiffness, and other parameters of the knee brace and obtained a more rational layout form of the knee brace. Conti et al. [7] introduced a design method focused on the overall collapse mechanism of seismic knee-braced frames. Li et al.[8]first proposed the knee braced frame system.This system is a new type of energy-consuming braced frame system, which has the advantages of large stiffness, low cost, simple repair and strong deformability. Under the action of medium or large earthquakes, the knee brace first yields and consumes energy. At this time, the main body of the beam and column is still in the elastic stage, so that the main body of the structure is not destroyed and easy to replace after the earthquake. Ji K H[9]a carried out experiments and finite element simulation. The results show that the knee brace has serious plastic deformation and the beam-column body is not damaged at this time, which verifies that the energy-consuming knee brace has good ultimate bearing capacity, elastic stiffness, ductility and hysteresis performance. H.-L.Hsu[10] carried out low cyclic quasi-static test on buckling restrained knee brace steel frame. The test results show that the arrangement of knee brace in steel frame structure can obviously improve the strength and stiffness of the structure, and make the structure have good deformation ability and energy dissipation ability, which changes the performance of traditional steel frame. Jia et al. [11] executed a design experiment to study a buckling-restrained brace composite frame system. The outcomes demonstrate that installing braces markedly improves the lateral stiffness, ultimate load-bearing capacity, and energy dissipation performance of the composite frame. Xie et al. [12] performed reverse loading tests on sandwich buckling restrained brace specimens with varying gaps. The test results confirmed that the structure possesses stable hysteretic performance and energy dissipation capacity, aligning with the specific values outlined in AISC2010. The compressive strength adjustment coefficient increases as the gap widens. However, the maximum number of cycles under large axial strain sees a significant reduction, leading to a decrease in energy dissipation capacity. Xu et al. [13–15] analyzed the buckling restrained knee-braced steel frame under unidirectional static and low cyclic loads. Xu et al. performed the modal and dynamic time-history analyses under three different seismic waves. The results show that the buckling restrained knee-braced steel frame has good seismic performance, and the arrangement of knee brace can effectively reduce structures' seismic response.

Following Refs. [16–25], the present paper studies the influence of BRKBs on the performance and failure mechanism of steel frame composite beam-column joints considering the floor effect. Thus, a BRKBJ and an ordinary beam-to-column rigid joint (BTCRJ) were selected for quasi-static tests under low cyclic loading and seismic performance analysis.

2. Experiment description

2.1. Specimen dimension design

In this experiment, the steel frame under horizontal seismic load was taken as the prototype and the composite beam-column rigid joint in the frame was selected as the experimental model. The distance between column inflection points, i.e., column height plus the distance between column's upper and lower hinge supports, is 2300 mm. The middle inflection point of the beam span is 1660 mm away from the outer edge of the endplate. The size of beam and column of the joints are H 350 × 172 × 7 × 12 mm, and H 300 × 300 × 12 × 16 mm, respectively. The lengths of the column and beam are 1780 mm and 2320 mm, respectively. The concrete floor is C30 with thickness and width of 70 mm and 1020 mm, respectively. The internal reinforcement is double-layer and double-direction, and HRB400 steel bars with 6mm@100 are used for longitudinal and transverse reinforcements. The stud is 16 cylindrical head stud,

the longitudinal spacing is 120 mm, and the transverse spacing is 100 mm. Accordingly, the BRKB is added. Note that the geometric size of the energy dissipation section of the knee brace core plate is 80 × 12 × 460 mm. To obtain the optimal joint performance, the arrangement angle of the knee brace is set parallel to the diagonal line of the frame with 770 mm from the beam end and 310 mm from the column bottom. The knee brace core plate is the Q235B steel with a low yield point, and the beam column is the Q355B steel. Beams and columns have H-shaped cross-sections and are rigidly connected with corner braces. The buckling restrained sleeve is added on both sides of the corner brace plate to prevent instability. The beam flange and column are connected by butt weld, which is fully melted groove welding, with the first-grade quality. Note that the welding material is manually welded by the E50 electrode. Also, the web bolt is connected by friction type of 10.9 grade M20 high strength bolt. The bolt hole diameter is 22 mm, the friction coefficient (μ) is 0.4, and the contact surface is sandblasted. The joint structure is shown in Fig. 1, and the BRKB structure is shown in Fig. 2.

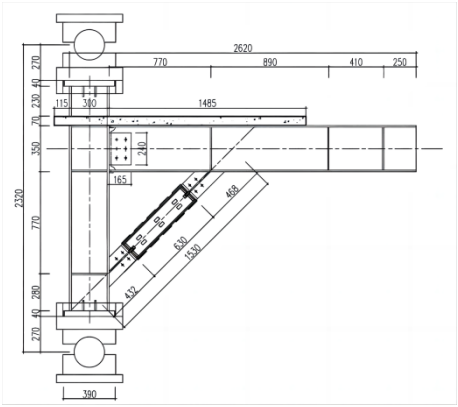

(a) BRKBJ size diagram

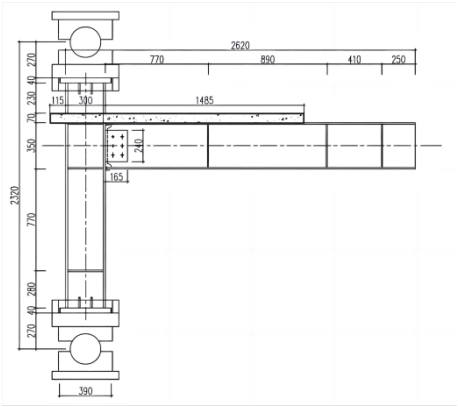

(b) BTCRJ size diagram

Fig. 1 Joint structure (unit: mm)

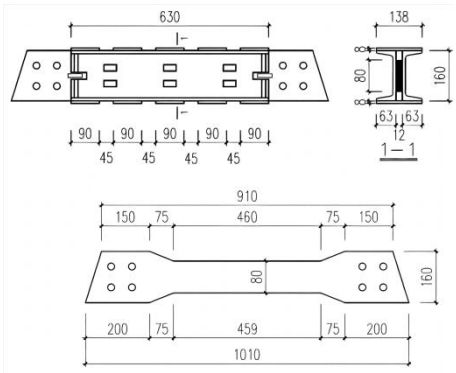

Fig. 2 BRKB structure (unit: mm)

2.2. Material properties test

The specimen thicknesses used in this test include 8 mm, 10 mm, 12 mm, and 14 mm. The thicknesses of Q355B steel are 8 mm, 10 mm, 12 mm, and 14 mm, and the thickness of Q235B steel is 12 mm. Three specimens were selected for each plate thickness with a total of 15 specimens. The test results of the specific mechanical properties are tabulated in Table 1. The mechanical properties of steel bar and concrete are provided in Table 2 and Table 3.

Table 1
Mechanical properties of steel materials.

Materials	*t*(mm)	f_y(N/mm^2)	f_u(N/mm^2)	*E*(N/mm^2)	δ(%)
Q355	8	367.2	455.8	196100	22.2
	10	304.4	469.6	200000	27.0
	12	380.1	539.6	204600	22.7
	14	330.4	472.7	206000	24.6
Q235	12	272.7	448.1	201400	32.3

Table 2
Mechanical properties of reinforcing steel

Material	Bar diameter	f_y(N/mm^2)	f_u(N/mm^2)
Steel bar	φ6	410.3	566.7

Table 3
compressive strength of concrete

Material	Strength grade	$f_{cu,k}$ (N/mm^2)	f_{ck}(N/mm^2)
Concrete	C30	31.38	20.98

2.3. Loading device

The loading device of this test is depicted in Fig. 3. Two vertical actuators are linked with the reaction frame, and a horizontal constraint is linked with the reaction wall. The reaction frame and the lateral constraint are connected to the ground by anchor bolts. The test was conducted by MTS to impose a low cyclic load on the beam end to observe the joint's failure process and to analyze the energy dissipation capacity. In preloading, the parts of the component were closely contacted to ensure the whole device's stability, reliability, and normal use. In formal loading, first, a constant vertical load of 830 kN was applied with a jack along the axial direction of the column top. The loading process, mainly composed of two stages, was adopted at the beam end. The first stage was the elastic stage, in which the components did not enter the yield state. In the elastic stage, the load was increased by integral multiples of 25 kN. When any cross-section reached the yield point, and the plastic deformation occurred, it entered the elastic-plastic stage, i.e., the second stage. At this time, the load was increased with integral multiples of yield displacement. Note that each load cycle was two weeks. When the bearing capacity of the specimen decreased to less than 85% of the ultimate bearing capacity or when a large deformation or failure occurred in the beam, column, and joint area, the loading was stopped, and the test was complete.

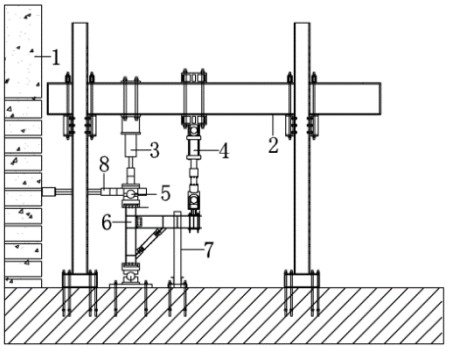

1-Reaction wall; 2-Reaction frame; 3-Column end vertical actuator; 4-Beam vertical actuator; 5-Ball hinge; 6-The specimen of knee brace joint; 7-Lateral constraint; 8- Horizontal constraint

(a) Test schematic diagram

(b) BRKBJ experimental device diagram

(c) BTCRJ experimental device diagram

Fig. 3 Test loading device diagram

2.4. Displacement meter and strain gauge layout

BRKBJ arrangement of 6 displacement meters, BTCRJ specimen arrangement of 5 displacement meters. The displacement meters No. 1 and No. 2 were used for monitoring the diagonal displacement of the beam and column joint domain. The displacement meter No. 3 was used to monitor the displacement of the beam end loading point. The displacement meters No. 4 and No. 5 were used for monitoring the displacement of column ends. The displacement meter No. 6 was used to monitor the axial tension and compression deformation displacement of the buckling restrained corner brace. The strain of the beam, column joint domain, corner brace, column intersection point, and the beam-column near the joint were observed. Note that the strain gauge numbers of both joints near the joint domain were the same. The displacement meter and the arrangement of key measuring points are illustrated in Fig. 4 and Fig. 5.

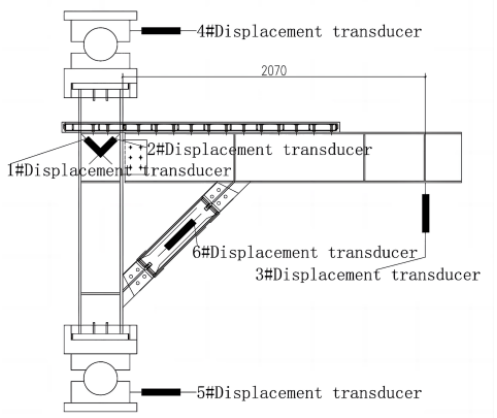

(a) BRKBJ displacement sensor layout

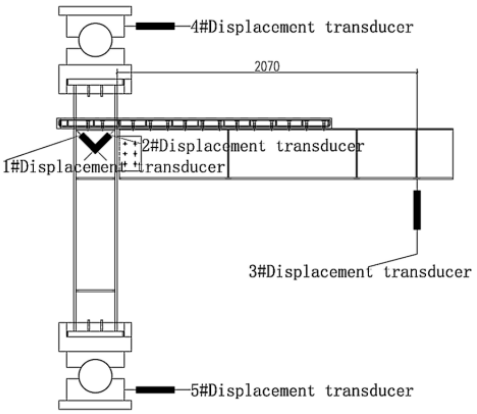

(b) BTCRJ displacement sensor layout

Fig. 4 Layout of displacement sensors of joints

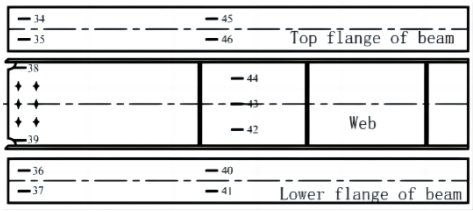

(a) Layout of strain gauges at beam's key position

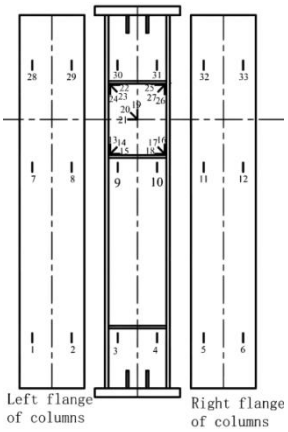

(b) Layout of strain gauges at columns' key positions

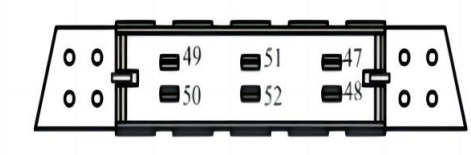

(c) Layout of strain gauges at BRKBs

Fig. 5 Layout of measuring points

3. Experimental process

3.1. BRKBJ pseudo-static test process

In the elastic loading stage, when the vertical load of 154.2 kN along the pressure direction was applied to the beam's end, the strain at the gauge No. 52 at the core of the buckling restrained corner brace reached 1358με , which is the maximum of all strains of the core. As shown in Fig. 6, It can be determined that the core material part yields at this time, and the yield strength is measured by the material performance test of the sample. After one loading cycle in the elastic loading stage, the maximum displacement along the beam's pressure direction was 7.6 mm. Thus, the yield displacement was 7.6 mm, and the yield load was 154.2 kN. The cyclic load was carried out with the integral multiple yield displacement, and each stage was loaded twice. As shown in Fig. 7, when the vertical displacement imposed by MTS at the beam end along the compressive direction reached 10.51 mm, the load at the beam end was 195.4 kN, and cracks appeared in the middle of the concrete slab. Also, when the displacement applied by MTS at the beam end along the compressive direction

reached 21.1 mm, the corresponding load was 290.71 kN, and the maximum strain of the reinforcement in the upper floor reached 1390. Thus, the reinforcement was expected to yield at this time. When the vertical displacement applied by MTS at the end of the beam along the compressive direction reached 24.13 mm, the load at the end of the beam reached 346.61 kN. The data monitoring reveals that the maximum strain measured by strain gauge No. 41 at the lower edge of the beam and corner brace is 1798 . Thus, the yield of the beam can be determined at this time. When the vertical displacement applied by MTS at the beam end along the compressive direction reached 32.34 mm, the load at the beam end was 333.38 kN. As shown in Fig. 8, the concrete slab detached from the steel column, and the penetrating cracks appeared in the middle of the slab. Fig. 9 shows that the fracture occurred in the middle of buckling restrained knee-braced core material when the load is up to 9 times the yield displacement. At this point, the connection between the beam and the corner brace yielded, while the beam end near the joint domain did not yield. When the load to the buckling restrained corner brace reached 11 times the upward yield displacement, a crack with a width of 8 mm appeared on the floor, the floor edge began to fall off, and the bearing capacity of the specimen decreased to less than 80%. At this point, the test is complete. The buckling restrained corner brace was broken, a large crack on the concrete slab and many penetrating cracks appeared, and the slab fell off. However, the beam and column were not damaged and unstable, and the beam-column joint domain maintained good mechanical properties, which was consistent with the two-stage yield design concept of the BRKBJ specimen.

Fig. 6 BRKBJ knee brace yield

Fig. 7 Crack on the concrete floor

Fig. 8 Crack on the concrete floor

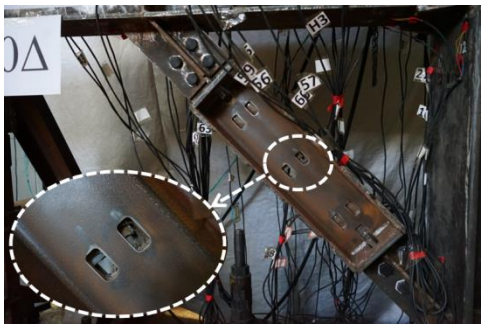

Fig. 9 BRKBJ core material failure

3.2. BTCRJ pseudo-static test process

Fig. 10 suggests that, in the elastic loading stage, when the force was loaded to 50 kN, cracks appeared near the joint domain of the floor and fell off. When the force was loaded to 140 kN along the pressure direction, penetrating cracks appeared near the joint domain of the floor. When a vertical load of 226 kN was applied in the direction of pressure, the strain at the root of the lower flange of the beam, at gauge No. 37, reached 1908 $\mu\varepsilon$, the maximum value recorded among all strains. Moreover, a clear inflection point appeared on the load-displacement curve of the beam endpoint. Thus, the yield of the beam can be realized at this time, which was after one loading cycle in the elastic loading stage. The load-displacement curve also shows that the maximum displacement of the beam endpoint along the pressure direction reached 20 mm. The yield displacement was 20 mm, and the corresponding yield load was 226 kN. It should be noted that 20 mm integral multiple yield displacements were used to increase the cyclic load amplitude. At each displacement stage, the loading cycle was imposed twice. When the vertical displacement along the pressure direction applied by MTS at the beam endpoint reached 28.74 mm, the load at the beam endpoint was 290.71 kN, and the maximum steel bar strain at the upper floor reached 1472 $\mu\varepsilon$. It can be realized that the steel bar yielded at this time. When the vertical displacement in the compression direction applied by MTS at the beam endpoint reached 60 mm, the load at the beam endpoint was 305.98 kN, and cracks appeared near the joint domain of the floor. When the load reached 4 times yield displacement, the lower flange of the beam near the joint domain buckled, and the load at the beam endpoint was 313.5 kN (Fig. 11). When the loading was up to 6 times the yield displacement, the lower flange and web of the beam near the joint domain were torn (Fig. 12). At this point, the test was terminated.

Fig. 10 Crack on the concrete floor

Fig. 11 Beam flange deformation

Fig. 12 Beam flange failure

4. Test result analysis

4.1. Load-displacement curve

The load-displacement hysteresis curves of both specimens are compared as depicted in Fig13-Fig14.

Before BRKBs fracture, the hysteresis curve of BRKBJ is shuttle-shaped and full, and it has good energy dissipation performance. In the early loading stage, due to the coupling effect of buckling restrained brace and beam-column, BRKBJ has greater stiffness than BTCRJ. The BRKBJ specimen's stiffness decreases with increasing the number of cycles in the displacement control stage. The hysteresis curve of the BRKBJ specimen has three distinct stages, which imply that the buckling restrained brace and beam-column yield successively. When the cycle reaches 9 times the yield displacement, the fracture occurred in the middle part of the core material, the bearing capacity of BRKBs decreased to 59.6 % of the ultimate bearing capacity. At this time, the main body of the beam and column maintained good integrity except the core material, indicating that BRKBs had good energy dissipation capacity. After that, the BRKBs were continuously loaded to 11 times the yield displacement, and the beam-column joints were loaded, indicating that the beam-column joint domain still had good energy dissipation capacity after BRKBs fracture. Overall, the hysteresis curve is "symmetrical" in the tension and compression directions, indicating that the influence of floor slab on the hysteretic behavior of buckling restrained corner braced joints is not significant.

The hysteresis curve of the BTCRJ specimen is relatively stable and full, and the specimen has large stiffness at the initial loading stage. With the increase of loading multiple, the stiffness decreases. When the cycle reaches five times the yield displacement, the total load of the load-displacement curve no longer increases, and the hysteresis loop shows a downward trend. The lower flange of the beam at the beam-column connection is torn, and the bearing capacity decreases to 58.3% of its ultimate bearing capacity. The hysteresis curve of the BTCRJ specimen is overall "asymmetric". The hysteresis curve in the tensile direction is fuller because the floor is in a tensile state when the beam ends are compressed. Once the concrete cracks and the steel bars yield, the floor fails. When the beam end is pulled, the floor and the concrete are in a pressurized state. Therefore, when the beam end displacement is large, the joint stiffness is obviously degraded in the compression direction, while the beam endpoints are in the tensile state and the concrete is still in the compression state.

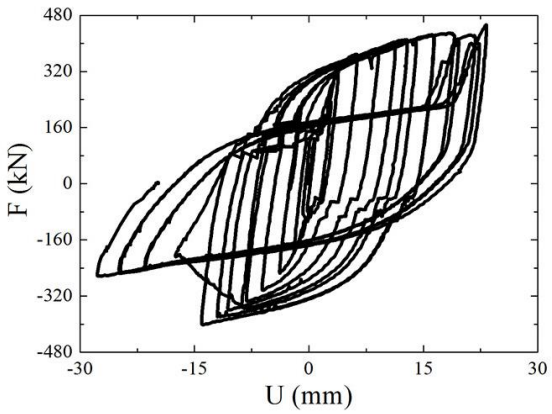

Fig. 13 Core material load - displacement curve

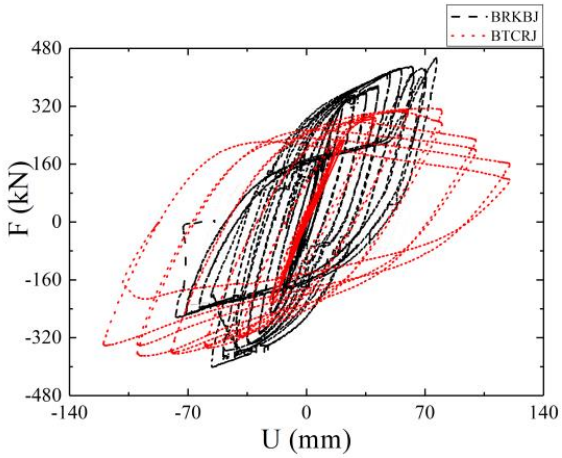

Fig. 14 Comparison of load-displacement curves of BRKBJ and BTCRJ specimens

4.2. Skeleton curve

The skeleton curves of both specimens are compared as illustrated in Fig. 15. The ultimate bearing capacity of the BRKBJ specimen is 453.73 kN. The skeleton curve of the specimen changes linearly before the buckling restrained corner core material yields. The whole specimen is in the elastic stage. After the core material yields, the skeleton curve has obvious bending. Meanwhile, with gradually increasing the displacement, the specimen stiffness gradually decreases. After the beam and column yield, the stiffness will decrease again. The skeleton curve has an obvious inflection point. When the BRKBJ specimen is loaded in the tensile direction to 9 times the yield displacement of the energy dissipation knee brace, the middle part of BRKBs fractured. Before the fracture of the core material. the displacement and stiffness in the tensile and compressive directions are symmetrical, indicating that the floor slightly influences the BRBKJ specimen's stiffness. The ultimate bearing capacity of the BTCRJ specimen is 342.14 kN, and the skeleton curve changes linearly before the beam and column yield. After the beam and column yield, the stiffness decreases significantly when the displacement in the compressive direction reaches 80 mm. However, the stiffness begins to decrease when the displacement in the tensile direction reaches 105 mm, indicating that the floor has a significant enhancement effect on the stiffness in the BTCRJ specimen's tensile direction. The loads and corresponding displacements of both specimens at each stage are shown in Table 3. It can be realized that setting BRKBs can effectively increase the yield displacement of beam and column, improve the yield strength, and effectively delay the cracking of concrete and the yield of steel bars. The ultimate bearing capacity increases by 32.6%, and the displacement decreases by 19.2% under ultimate load.

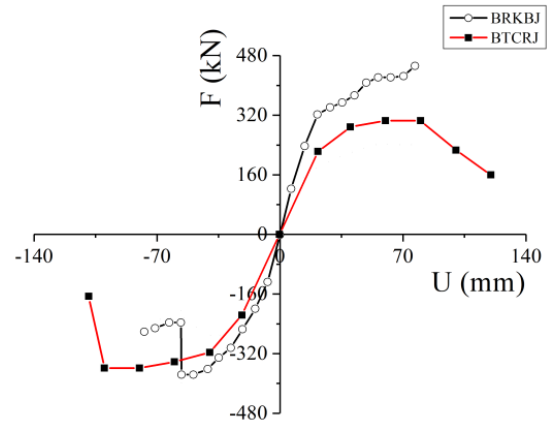

Fig. 15 Comparison of skeleton curves of BRKBJ and BTCRJ specimens

Table 3
Core material, beam-column yield displacement and load.

Specimen	Core yield		concrete crack		Beam-column yield		limiting condition	
	Δ_c	F_c	Δ_f	F_f	Δ_y	F_y	Δ_u	F_u
BRKBJ	7.55	154.21	11.42	195.4	24.13	346.6	78.83	453.7
BTCRJ	-	-	4.26	50	19.95	222.1	93.97	342.1

4.3. Stiffness degradation curve

Note that the secant stiffness (Ki) represents the specimen stiffness under low cyclic loading. The stiffness degradation curves of both specimens are compared as provided in Fig. 16， the curves of both specimens are relatively smooth before the BRKB yields. The BRKBJ specimen has the characteristics of large stiffness and small displacement. After the displacement increases to the failure point of the knee brace, the stiffness in the tensile direction decreases rapidly, and the stiffness degradation in the compression direction is still gentle. This is because the knee brace fails when the beam end is tensioned, while the knee brace in the compression direction is still in function due to the existence of the buckling restrained sleeve. When the BRKBJ specimen reaches the ultimate bearing capacity state, it still maintains 42% of the initial stiffness, indicating that the BRKB is arranged based on the rigid connection of the beam and column. Note that it can meet the requirements of seismic fortification. For BTCRJ, with the increase of load displacement, the degradation trend in the tensile direction is smaller than that in the compressive direction. This is because even if the concrete cracks and the steel bars yield, the floor slab can partially provide stiffness when the beam ends are pulled. When the specimen reaches the ultimate bearing capacity state, the specimen has an initial stiffness of about 41%.

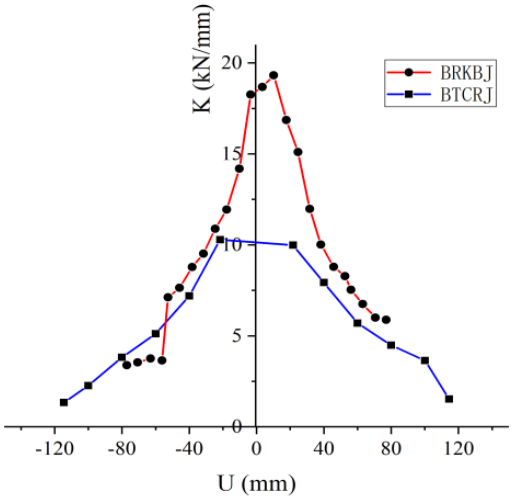

Fig. 16 Contrast diagram of stiffness degradationcurve of two specimens

4.4. Ductility analysis

The equivalent viscous damping coefficient (he) is used to determine the joint's energy dissipation capacity, and the displacement ductility coefficient (μ) is used to determine the structure ductility. These coefficients of both specimens are tabulated in Table 4.

Table 4
Equivalent viscous damping and displacement ductility coefficients

Specimen	BRKBJ	BTCRJ
he	0.387	0.338
μ	7.3	6.0

The structure ductility is one of the important indexes to evaluate the structure's seismic performance. In this test, both joint specimens were destroyed before the bearing capacity decreased to 85% of the ultimate bearing capacity. Thus, the specimen displacement was taken when the maximum bearing capacity was reached. The seismic ductility coefficient of the frame structure specified in the code is 4.0, and the displacement ductility coefficient of both specimens meets the code requirements. The equivalent viscous damping coefficient and displacement ductility coefficient of the buckling restrained corner braced joint are increased by 14.5% and 21.6%, respectively, indicating that the buckling restrained corner braced joint has good ductility performance.

The greater the equivalent viscous damping coefficient, the better the energy dissipation capacity of the specimen. Among them, BRKBJ specimens take the hysteretic loop calculation when the beam and column just enter the yield after the yield of the energy dissipation core material, and BTCRJ takes the hysteretic loop calculation when the beam and column just enter the yield.

4.5. Strain analysis of key positions

The strain changes of the measuring points 7 and 28 at the left flange and 11 and 32 at the right flange are illustrated in Fig. 17.

The comparative analysis reveals that the strain of the flange on both sides of the column in the elastic stage is small enough to meet the requirements of the strong column design. For the BTCRJ specimen, the beam end is not fully relaxed when the axial force of the column end is applied. Thus, it partially impacts the strain of the column flange. With increasing the load, the strain increasing trend of the BRKBJ specimen is less than that of the BTCRJ specimen. It shows that the buckling restrained corner brace can share the load at the end of the column in the traditional beam-column frame joint. Furthermore, the buckling restrained corner brace can reduce the effect of load on the column, and change the mechanical performance of the traditional beam-column frame joint. Under reciprocating load, the lower flange at the connection between the beam and the corner brace experiences a bending instability, while the column still maintains good performance and no instability occurs. These observations illustrate that the strategic placement of buckling restrained braces can shift the joint's plastic hinge outward to the joint between the brace and the beam, thereby fulfilling seismic design requirements.

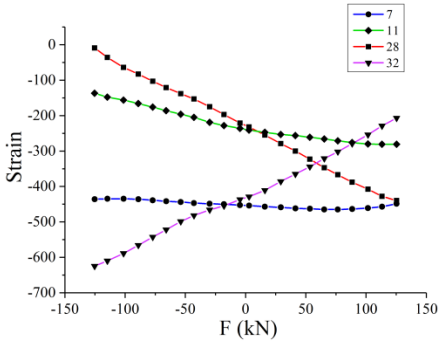

(a) BRKBJ column flange strain

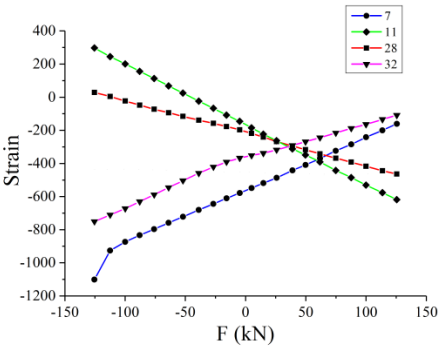

(b) BTCRJ column flange strain

Fig. 17 Strain contrast diagram on the wing edge of a column

The strain changes of measuring point 5 at the connection between the column and the knee support of the BRKBJ specimen, measuring point 41 at the connection between the beam and the knee support, and measuring point 37 at the beam endpoint near the joint domain are plotted in Fig. 18.

The yield load at the connection between beam and knee brace support of the BRKBJ specimen is significantly greater than that at the beam end of the BTCRJ specimen. At this time, no yield occurs at the connection between the column of the BRKBJ specimen and the knee brace support and near the joint domain. This phenomenon can indicate that the layout of BRKBs can effectively absorb energy. In the later loading stage, the knee braces and the beam near the connection of knee braces take energy. Thus, not only the yield-load curve of the whole beam and column is improved, but also the formation of plastic hinges at the beam end near the joint domain is prevented. Therefore, the overall energy dissipation capacity of the whole joint domain is improved.

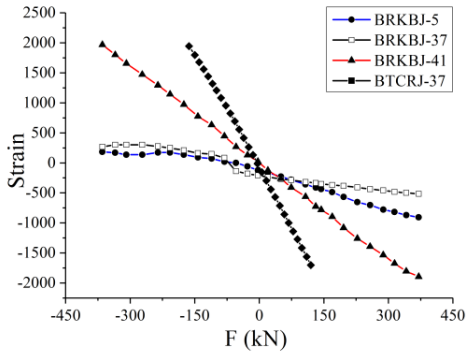

Fig. 18 The yield-strain curves of BRKBJ and BTCRJ specimens

The strain changes of the five measuring points 14, 17, 20, 23, and 27 in the joint domain of both specimens are presented in Fig. 19.

In the elastic stage, the strain in joint domains of both specimens change linearly, while the strain change trend of the BRKBJ specimen is significantly less than that of the BTCRJ specimen. This fact indicates that adding the buckling restrained corner brace can significantly reduce the stress level in the joint domain, ensure the stiffness of the joint domain, avoid large shear deformation in the joint domain of the specimen, and meet the design requirements of strong joints.

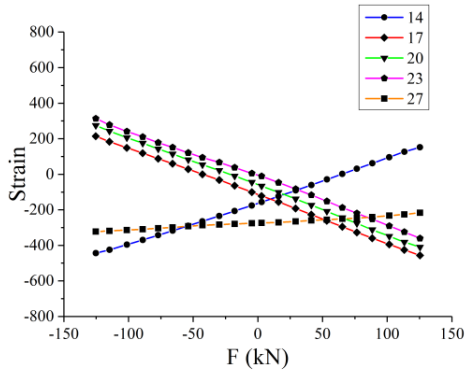

(a) BRKBJ strain in the joint domain

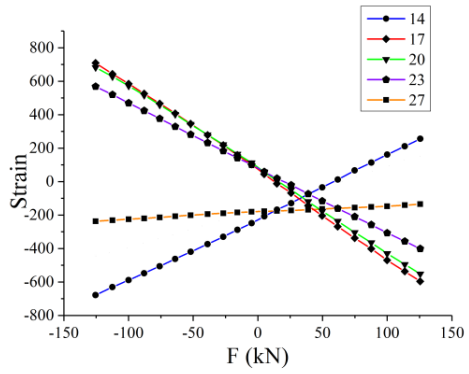

(b) BTCRJ strain in the joint domain

Fig. 19 Strain contrast diagram in the column joint domain

5. Conclusion

The seismic performance of the traditional steel composite beam-column rigid joint and the BRKBJ considering the influence of the floor slab was explored. A BRKBJ and a BTCRJ were selected for quasi-static tests under low cyclic loading and for seismic performance analysis. Moreover, the failure mode, bearing capacity, hysteresis performance, and ductility of both joints were analyzed. Our study has led us to the following conclusions:

(1) It was determined that the incorporation of a BRKB into the BTCRJ specimen led to a 32.6% increase in the BRKBJ specimen's ultimate load-bearing capacity. The displacement is reduced by 19.2% when the ultimate bearing capacity is reached. When the ultimate bearing capacity is reached, the initial stiffness remains about 42%, the yield displacement of beam and column increases slightly, the yield load is greatly improved, and the mechanical performance of the joint is improved.

(2) The hysteresis curve of the BRKBJ specimen is robust. Compared to BTCRJ, BRKBJ exhibits a 14.5% increase in the viscous damping coefficient, and a 21.6% increase in the ductility coefficient. Under cyclic loading, the BRKBJ specimen displays superior symmetry and heightened load-bearing capacity. This suggests that the use of buckling restrained braces can enhance the energy dissipation capacity of composite joints and also improve seismic performance.

(3) The layout of the floor slab has minimal impact on the BRKBJ specimen under seismic activity. The joints present almost equal energy dissipation and stiffness in both tension and compression directions. Additionally, the floor slab can significantly enhance the stiffness and energy dissipation capacity of the beam end under tension after the beam and column yield. However, the effect of the floor slab in the compression direction is not obvious.

(4) The BRKBJ specimen has a two-stage yield. First, the core material of the buckling restrained corner brace and the main part of the beam and column yield. When the plastic failure occurs, the increase of buckling restrained corner brace can move the plastic hinge of the beam end of the traditional beam-column joint to the connection between the corner brace and the beam. Moreover, the buckling restrained corner brace reduces the stress level of the joint domain and improves the energy dissipation capacity of the joint domain under seismic action.

Acknowledgement

The research was funded by the Ministry of Housing and Urban-Rural Development(No. 2018-K5-001), the Natural Science Foundation of Liaoning Province (2019-ZD-0664) and the Department of Education of Liaoning Province (No. LNJC202005), which is gratefully acknowledged.

References

[1] Hsu H L, Li Z C. Seismic performance of steel frames with controlled buckling mechanisms in knee braces[J]. Journal of Constructional Steel Research, 2015, 107: 50-60.
[2] Junda E, Leelataviwat S, Doung P. Cyclic testing and performance evaluation of buckling-restrained knee-braced frames[J]. Journal of Constructional Steel Research, 2018, 148: 154-164.
[3] Yin Z Z, Feng D Z, Yang B, et al. The seismic performance of double tube buckling restrained brace with cast steel connectors[J]. Advanced Steel Construction, 2022, 18(1): 436-445.
[4] Chen Z Y, Ge H B, Usami T. Analysis and design of steel bridge structures with energy absorption members[J]. Advanced Steel Construction, 2008, 4(3): 173-183.
[5] Zhou D M. Influential analysis of changing parameters of the knee brace on seismic performance of steel story-adding structure[J]. Engineering Construction, 2017,49（4）:1-7. (in Chinese))
[6] Zhou D F. Analysis on seismic performance of the knee brace in steel story- adding structure[D]. Shandong. Qingdao Technological University, 2016. (in Chinese))
[7] Conti M A, Mastrandrea L, Piluso V. Plastic design and seismic response of knee braced frames[J]. Advanced Steel Construction, 2009, 5(3): 343-366.
[8] Li Q S, Huang Z, Chen L Z. Elastic-plastic analysis of braced frame system with inclined corner bracing [J]. Industrial Buildings, 2005,35 (5) : 85-87.
[9] JI K H.Study on seismic behavior of steel frame with corner braces [D].Nanjing University of Technology, 2006.
[10] H.-L.Hsu,Z.-C.Li. Seismic performance of steel frames with controlled buckling mechanisms in knee braces[J]. Journal of Constructional Steel Research, 2015,(107):50-60.
[11] Jia M M, Li L, Hong C, et al. Experiment of hysteretic behavior and stability performance of buckling-restarined braced composite frame[J]. Advanced Steel Construction, 2021, 17(2): 149-157.
[12] Xie L, Wu J, Shi J, et al. Influence of the core-restrainer clearance on the mechanical performance of sandwich buckling-restrained braces[J]. Advanced Steel Construction, 2020, 16(1): 37-46.
[13] Xu F, Wang X Z. Seismic Performance for Steel Frames with Different Layouts of Knee Brace[C]. Proceedings of The 2016 International Conference on Architectural Engineering and Civil Engineering, 2016(72); 624-627.
[14] Xu F, Gong T B, Jia L G. Seismic performance of steel frame beam-column connection with single-braced energy dissipative joint[C]. National Forum of Civil Engineering Graduates in Green Construction and Industrialization, 2015. 12. (in Chinese))
[15] Gong T B. Study on seismic performance of buckling-constrained concrete braced steel frame[D]. Laoning, Shenyang Jianzhu Univesity, 2017. 3. (in Chinese))
[16] WANG Yan, FENG Shuang, WANG Yutian. Experimental study on hysteretic behavior for rigid-reinforced connections[J]. China Civil Engineering Journal, 2011, 4(5): 57-68. (in Chinese))
[17] ZHAO Junxian, YU Haichao, PAN Yi. Seismic performance of sliding gusset connections in buckling-restrained braced steel frame[J]. Journal of Building Structures, 2019, 40（2）; 117-127. (in Chinese)
[18] Jia B, Zhang Q L, Luo X Q. Study on hysteretic behavior of aluminum alloy energy dissipation braces[J]. Journal of Building Structures, 2015, 36(08): 49-57. (in Chinese))
[19] Jinkoo Kim, Youngill Seo. Seismic design of steel structures with buckling-restrained knee braces [J]. Journal of Constructional Steel Research, 2003.59(12)： 1477-1497.

[20] Amador Tera´n-Gilmore, Jorge Ruiz-Garcı´. Comparative seismic performance of steel frames retrofitted with buckling-restrained braces through the application of Force-Based and Displacement-Based approaches [J]. Soil Dynamics and Earthquake Engineering, 2010.
[21] Qu Z ,Xie J Z, Wang T, Shoichi Kishiki. Seismic retrofit design method for RC buildings using buckling-restrained braces and steel frames [J]. Engineering Structures, 2017. 139: 1-14.
[22] Hamdy Abou-Elfath, Mostafa Ramadan, Fozeya Omar Alkanai. Upgrading the seismic capacity of existing RC buildings using buckling restrained braces [J]. Alexandria Engineering Journal, 2017. 56(2): 251-262.
[23] Fatih Sutcu, Toru Takeuchi, Ryota Matsui. Seismic retrofit design method for RC buildings using buckling restrained braces and steel frames [J]. Journal of Constructional Steel Research, 2014. 101: 304-313.